JCTC Journal of Chemical Theory and Computation

Theoretical Studies on Optical and Electronic Properties of Propionic-Acid-Terminated Silicon Quantum Dots

Q. S. Li,[†] R. Q. Zhang,*[,†] T. A. Niehaus,[‡,§] Th. Frauenheim,[‡] and S. T. Lee[†]

Centre of Super-Diamond and Advanced Films (COSDAF) and Department of Physics and Materials Science, City University of Hong Kong, Hong Kong SAR, China, Bremen Center for Computational Material Science, University Bremen, 28334 Bremen, Germany, and Department of Molecular Biophysics, German Cancer Research Center, D-69120 Heidelberg, Germany

Received February 19, 2007

Abstract: The origin and stability of photoluminescence (PL) are critical issues for silicon nanoparticles to be used as biological probes. Optical and electronic properties of propionic-acid (PA) -terminated silicon quantum dots (SiQDs) were studied using the density-functional tight-binding method. We find that the adsorbed PA molecules slightly affect the structure of silicon core. The PA adsorption does not change the optical properties of SiQDs, while it substantially decreases the ionization potentials in the excited state and results in some new active orbitals with adjacent energies around the Fermi energy level. Accordingly, the modified surface of SiQDs can serve as a reaction substrate to oxygen and solvent molecules, which is responsible for the increase in both PL stability and water solubility.

1. Introduction

Silicon is the leading semiconductor material in microelectronic industry.[1] At nanometer sizes, a very important feature of the material is the enormous surface area to volume ratio.[2] Modification or functionalization of the nanoscale silicon surface might open the possibility of integrating solid-state electronics with optical sensing techniques.[3−6]

Due to the well-known quantum confinement effect, silicon quantum dots (SiQDs) possess novel optical properties that can potentially be exploited to make optoelectronic devices[7−11] and new biological chromophores.[12−15] Unfortunately, this promise is hampered by the easiness of surface oxidation of free-standing SiQDs. It is found that hydrogen-terminated SiQDs exhibit strong PL in the blue region of visible spectrum, but their surface oxidized easily at room temperature,[16] and this oxide surface passivation leads to a dipole-forbidden yellow-red emission.[17]

Besides good photoluminescence (PL) stability, good water solubility is also essentially required for silicon nanocrystals to be employed for bioimaging.[18] Actually, the hydrogenated SiQDs have poor dispersibility in water and some other common solvents. For this reason, much experimental work[9,19−28] has been carried out on surface functionalization of SiQDs.

For instance, Warner and co-workers[20] attached allylamine to silicon particles using a Pt catalyst. The allylamine-capped SiQDs are water-soluble and exhibit strong blue PL with a rapid rate of recombination. In contrast, Li and Ruckenstein[21,22] added acrylic acid on the SiQDs surface by a UV-induced graft method and alleged the potential of produced propionic-acid (PA) -terminated SiQDs as biological staining agents with tremendous photostability. The high density of carboxylic acid moieties can be used to covalently immobilize molecules containing amines groups, such as proteins.[29,30] In a subsequent contribution, water-dispersible PA-terminated SiQDs were prepared by photoinitiated hydrosilylation.[23] Sato and Swihart[23] demonstrated that the strongpoint of their experiment is that the SiQD size and corresponding PL emission color changing continuously from yellow to green could be controlled by varying the etching time, while other water-dispersible particles in previous reports[20−22] only exhibit a single emission color.

* Corresponding author e-mail: aprqz@cityu.edu.hk.
[†] City University of Hong Kong.
[‡] University Bremen.
[§] German Cancer Research Center.

10.1021/ct700041v CCC: $37.00
Published on Web 06/09/2007

As stated above, the surface modification of SiQDs has been the subject of numerous experimental investigations. Yet, as far as we know, there are only a few theoretical studies[31−35] on electronic structure and optical properties of functional group-terminated SiQDs up to date. Early in 1996, one of the present authors and his co-workers have pointed out the importance of surface saturation on the stability of silicon nanostructures.[31] In 2005, Reboredo and Galli[34] reported that steric repulsion is dominant in determining the stability of alkyl-passivated clusters. It is also concluded that alkyl passivation weakly affects optical gaps of SiQDs, while it substantially decreases ionization potentials and electron affinities.[34] Recently, the excited-state properties of allylamine-capped SiQDs have been theoretically studied in our group.[35] The calculation results verified that allylamine is a good protecting molecule, as it reduces the surface oxidation possibility and maintains optical properties of SiQDs in the visible region.[35] However, the physical mechanism and chemical nature responsible for the optical properties of water-soluble luminescent SiQDs are far from fully understood and still need further investigation.

In this work, a systematic theoretical study on the electronic structures and optical properties of PA-terminated SiQDs is presented as a function of adsorbed PA amounts. The obtained results will be compared with related experimental[9,19−28] and theoretical[31−35] results. We expect that the present work could reveal the main changes in structure and properties induced by surface modifications with organic molecules and thus provide new insights and guidance to the experimentalists. Particular efforts will be made to characterize the physical mechanism responsible for the optical properties, especially the luminescence, because the application of nanoparticles depends on their luminescence upon insertion into biological cells.

2. Computational Details

In this study, the self-consistent charge density-functional-based tight-binding approach, SCC-DFTB, and its time-dependent linear response extension TD-DFTB were employed to study the electronic and optical properties of selected hydrogenated and PA-terminated SiQDs. The DFTB method has been described in detail elsewhere[36−40] and will be outlined here only briefly.

The SCC-DFTB model was derived from a second-order expansion of the density functional theory (DFT) total energy functional with respect to the charge-density fluctuations, and the Hamiltonian matrix elements are calculated with a two-center approximation, which are tabulated together with the overlap matrix elements with respect to the interatomic distance.[36,37]

The TD-DFTB method[38] following the TD-DFT route of Casida[39,40] is capable of efficiently handling excited-state calculations of large systems. In excited-state energy calculations, a self-consistent field (SCF) calculation is conducted first to obtain the single-particle Kohn−Sham (KS) orbitals and the corresponding KS energies ϵ_i. Then, a coupling matrix which gives the response of the SCF potential with respect to a change in the electronic density is obtained as follows

$$K_{ij\sigma,kl\tau} = \sum_{\alpha\beta} q_{\alpha}^{ij} q_{\beta}^{kl} [\gamma_{\alpha\beta} + (2\delta_{\sigma\tau} - 1) m_{\alpha b}]$$

where δ and m respectively represent the charge-density fluctuations and the magnetization; σ and τ are spin indices; q represents the Mulliken charge; i and k are indices of the occupied KS orbitals, whereas j and l are unoccupied ones. The exchange-correlation energy has been included in the γ and m. The excitation energy (ω_I) is obtained by solving the following eigenvalue problem

$$\sum_{ij\sigma} [\omega_{ij}^2 \delta_{ik}\delta_{jl}\delta_{\sigma\tau} + 2\sqrt{\omega_{ij}} K_{ij\sigma,kl\tau} \sqrt{\omega_{kl}}] Fij\sigma^I = \omega_I^2 F_{kl\tau}^I \quad (\omega_{ij} = \epsilon_{j-} \epsilon_i)$$

where F denotes a normalized spherical density fluctuation. The total energy of the excited state is given as a sum of ground-state energy E_{GS} and the excitation energy ω_I:

$$E_{I\Sigma} = E_{GS} + \omega_I$$

According to Kasha's rule, optical emissions always occur from the lowest state. For all the SiQDs studied here, the lowest singlet−singlet transition is optically allowed. Therefore, attention will be paid to the structure changes and properties related to the first singlet excited state (S_1 state). In the following section, the excited state refers to the S_1 state except when otherwise stated.

Additionally, in the present work, we used a basis of numerically described s, p, and d atomic orbitals for Si atoms, s and p atomic orbitals for C, N, and O atoms, and an s atomic orbital for H atoms.

To validate the reliability of the DFTB method, test calculations were performed for Si_5H_{12} and $Si_{35}H_{36}$. Our calculated absorption gap of Si_5H_{12} (6.40 eV) is close to the experimental value (6.5 eV)[41] as well as other high-level ab initio results.[42] For $Si_{35}H_{36}$, our optical gap (4.37 eV) compares well with MR-MP2 result (4.33 eV).[42] The above tests indicate that the accuracy of TD-DFTB is comparable with the high-level ab inito calculations to study the silicon nanostructures.

3. Results and Discussion

3.1. Geometrical Structures. The optimized ground-state geometries of hydrogenated and PA-terminated SiQDs are shown in Figure 1. We chose $Si_{35}H_{36}$ as the initial model because its diameter 1.1 nm is close to the experimental value,[20−23] and numerous related theoretical studies[17,32,35,43−50] have used the same model. Thus, it is convenient to compare the obtained results, such as structural parameters and optical gaps, with the corresponding values in previous experimental or theoretical studies. Our calculations confirmed that ground-state $Si_{35}H_{36}$ is in T_d symmetry. The Si−Si bond lengths are about 2.33−2.37 Å, and the bond lengths of the inner atoms are a little longer than those on the surface. The Si−H bond length is about 1.50 Å, which is in good agreement with the experimental value 1.48 Å.[51]

Like allylamine-capped SiQDs,[35] PA-terminated SiQDs favor adopting high symmetries, such as D_{2d}, S_4, and C_2. We chose to maximize the distance between passivants at

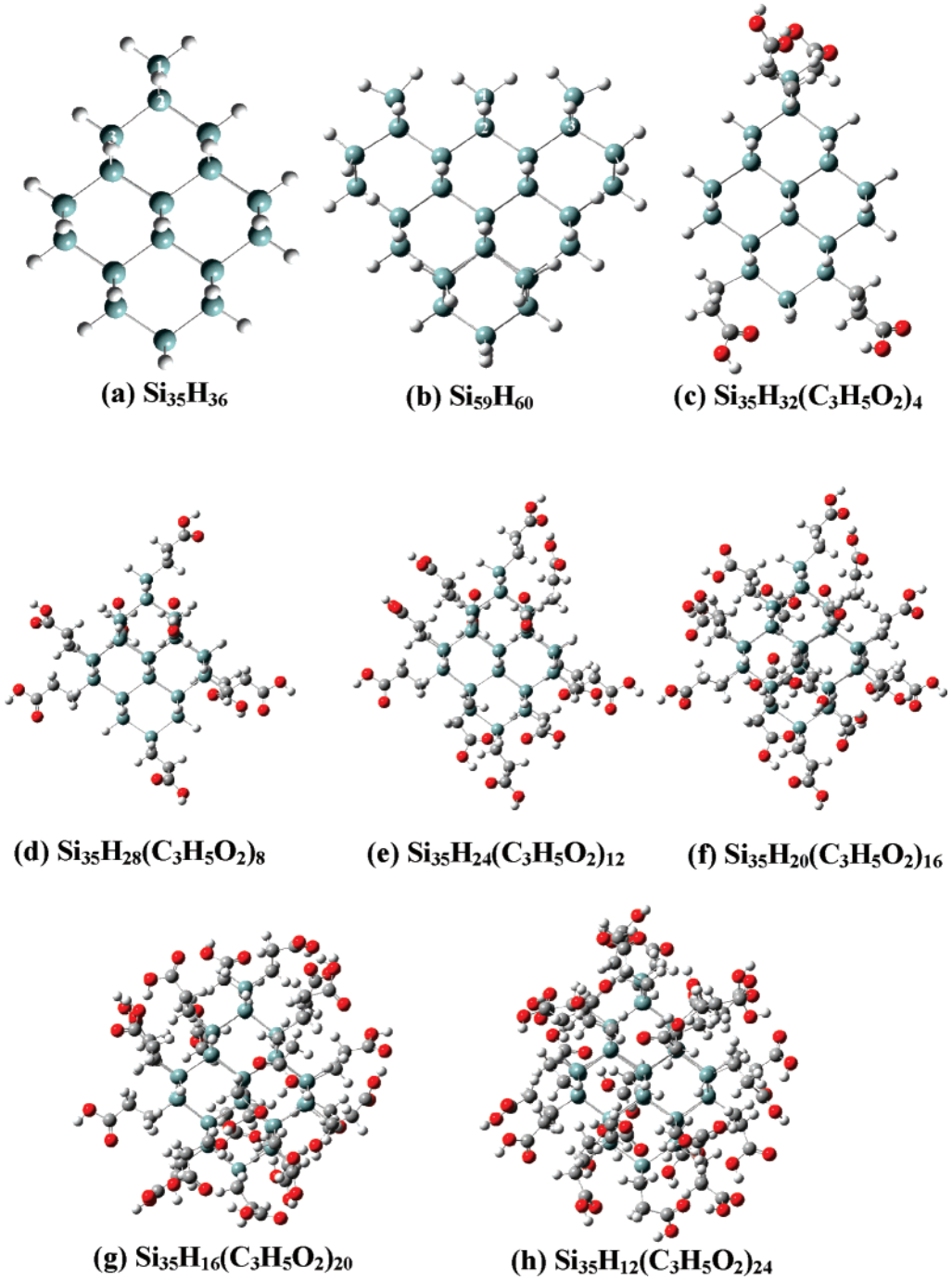

Figure 1. The optimized ground-state structures of SiQDs. The silicon, carbon, hydrogen, and oxygen atoms are cyan, gray, white, and red, respectively. The three different adsorption positions are labeled by number 1, 2, or 3 in (a) and (b).

the surface, to minimize steric repulsions. The optimized symmetrical structures were confirmed to be minimum points by vibrational frequency calculations that give all real frequencies. In the optimized structures, the amount of adsorbed PA molecules varies from 0 to 24. Note that there are likely many isomers for partly PA-terminated SiQDs, and the structures we discussed are the most minimum points in energy among all the isomers. We attempted to optimize the structures of fully PA-terminated SiQDs, that is, $Si_{35}(C_3H_5O_2)_{36}$, but the minimum-point search does not converge at all. This indicates that it is very difficult to make the surface of $Si_{35}H_{36}$ fully PA-terminated due to steric hindrance. This supposition was confirmed by FTIR spectroscopy[23] of PA-terminated SiQDs which showed that surface oxidation occurred during ultrasonication. In addition, our result is consistent with the previous theoretical finding that steric repulsion prevents full alkyl passivation of SiQDs with unreconstructed surfaces.[34] Note that the Si−Si or Si−H bond length of PA-terminated SiQDs is slightly longer than that in $Si_{35}H_{36}$, which indicates that the PA adsorption causes only small changes on the geometrical structure of the silicon core.

The most striking change in structure is usually associated with electronic excitation. Upon excitation, the T_d symmetry of $Si_{35}H_{36}$ cluster is broken down, resulting in a distortion in structure. The distortion leads to some Si−Si bonds

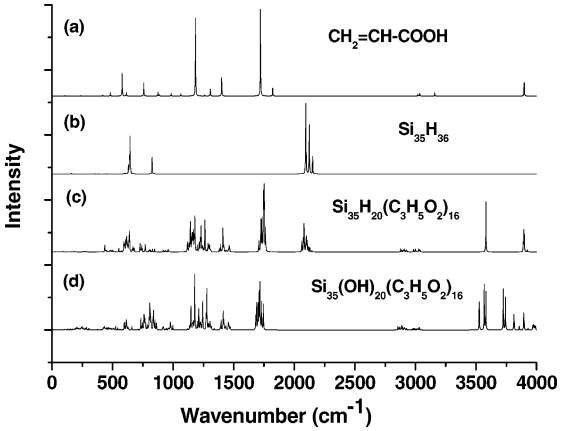

Figure 2. Calculated IR spectrum of acrylic acid, $Si_{35}H_{36}$, $Si_{35}H_{20}(C_3H_5O_2)_{16}$, and $Si_{35}(OH)_{20}(C_3H_5O_2)_{16}$.

increasing, while most of the Si−H bonds remain unchanged. The largest increase of Si−Si distance is up to 0.43 Å. Our calculations alleged that both hydrogenated and PA-terminated SiQDs are in C_1 symmetry in the S_1 state. Similarly, Luppi et al.[43] had verified that electronic and geometrical properties of silicon nanoclusters obtained by keeping the symmetry constraint for excited-state calculations are far from the actual energy minimum and lead to a wrong geometry and charge density of the excited state.

In order to gain more information about PA-terminated SiQDs, we simulated the IR spectrum of acrylic acid, $Si_{35}H_{36}$ and $Si_{35}H_{20}(C_3H_5O_2)_{16}$ (see Figure 2). For $Si_{35}H_{36}$, the peaks that appeared ranging from 2097 cm^{-1} to 2153 cm^{-1} are attributed to the strong Si−H stretching vibration. The Si−H bending mode leads to a very obvious peak at 644 cm^{-1}. Experimentally, these two vibrational modes were found at 2085 cm^{-1} and 631 cm^{-1}, respectively.[51] The peak at 827 cm^{-1} is attributed to the scissor vibration of the H−Si−H group. The absorption positions of Si−Si bonds are at the side lower than 500 cm^{-1}, with very weak peak intensity. The bonding of PA on the surface of the SiQDs is reflected by the peak at about 1250 cm^{-1} for the Si−CH_2 stretching vibration. The symmetric and asymmetric vibrations of C−CH_2 and C−COOH lead to the absorption between 2700 cm^{-1} and 3900 cm^{-1}. As shown in Figure 2(c), the vibrational spectrum of $Si_{35}H_{20}(C_3H_5O_2)_{16}$ is similar to the experimental spectrum,[23] except for the Si−H characteristic absorption peaks around 2100 cm^{-1} and 650 cm^{-1}. Considering the space steric effects, it is impossible to substitute all surface H atoms with PA molecules, so the absence of vibrational absorption of Si−H bonds in experiments possibly results from the oxidation of a small amount of unsubstituted H atoms. Then we simulated and showed the vibrational spectra of $Si_{35}(OH)_{20}(C_3H_5O_2)_{16}$ in Figure 2(d), which is in reasonable agreement with the experimental result.[23] This supports the conclusion that the PA adsorption decreases the oxidation rate of the SiQDs surface.

3.2. Optical Properties. According to the topological structure of $Si_{35}H_{36}$, there are three different positions on its surface (denoted by 1, 2, and 3 in Figure 1(a)). For comparison, the binding energies, HOMO−LUMO energy gaps, absorption energies of the SiQDs, and the net Mulliken charges of the PA molecule adsorbed on different positions

Table 1. Binding Energies, HOMO−LUMO Energy Gaps, and Absorption Energies of Single PA-Terminated SiQDs on Different Adsorption Positions of $Si_{35}H_{36}$ or $Si_{59}H_{60}$[a]

adsorption position	*E*(binding) (eV)	*E*(HOMO−LUMO) (eV)	*E*(absorption) (eV)	Mulliken charge of PA
		$Si_{35}H_{36}$		
1	2.194	4.306	4.345	−0.07
2	2.132	4.269	4.330	−0.06
3	2.155	4.287	4.299	−0.06
		$Si_{59}H_{60}$		
1	4.428	3.549	3.599	−0.07
2	4.396	3.550	3.594	−0.06
3	4.394	3.551	3.591	−0.06

[a] The different adsorption positions are labeled in Figure 1. The net Mulliken charges of the PA branch are also presented.

are presented in Table 1. In detail, there is a little amount of negative charge on the PA branch chain due to its receiving electrons from the silicon cluster. This can be ascribed to the moderately higher electronegativity of carbon (2.55) compared to silicon (1.90).[53] With the expansion of the silicon core from Si_{35} to Si_{59}, the HOMO−LUMO gap and absorption gap decrease by about 0.7−0.8 eV due to the quantum confinement effect, while the data are still independent of the adsorption position. In general, there is no obvious difference found in the binding energy, HOMO−LUMO energy gap, absorption energy, and net Mulliken charge of the branch. This indicates that the SiQDs are nearly isotropic, that is, the adsorption positions affect the optical properties to such a small degree that they could be ignored in the following study.

Identifying the first allowed optical transition in the case of large clusters is an important but difficult task, because in this case the absorption and emission spectra became quasicontinuous. In many cases, theoretical calculations do not evaluate oscillator strength and cannot explicitly identify optically allowed and dark transition. In the references where the oscillator strength is considered, the optical gap is usually defined as the point at which the integrated oscillator strength is nonzero or exceeds a threshold value. In the present work, we set the threshold value at 10^{-4} of the total oscillator strength. The chosen value of 10^{-4} stands above the level of numerical "noise" but is sufficiently small as to not suppress the experimentally detectable dipole-allowed transitions. The same definition for the optical gap has been used in previous experimental[54] and theoretical[45] work. Besides the optical gap, we pay special attention to the maximal peak position on the absorption or emission spectrum, since in many cases the maximal peak position is not corresponding to the optical gap but evident on the spectrum.

Table 2 presents our calculated HOMO−LUMO energy gaps, the maximal peak positions of absorption and emission, and corresponding oscillator strengths for hydrogenated and PA-terminated SiQDs. In Table 2, we can see that our calculated absorption energy for $Si_{35}H_{36}$ is 4.37 eV (283.8 nm), which is close to the recently reported TDDFT/B3LYP value 4.42 eV[48] and MR-MP2 result 4.33 eV.[42] After surface modification, the HOMO−LUMO energy gap decreases remarkably with an increase in the adsorbed molecules in ground-state or excited-state configuration, while the emis-

Table 2. HOMO−LUMO Energy Gaps,[a] the Maximal Absorption and Emission Wavelengths, and the Oscillator Strengths[b]

	ΔE_1 (eV)	absorption (nm)	f_1	ΔE_2 (eV)	emission (nm)	f_2
$Si_{35}H_{36}$	4.316	283.8	0.08	2.588	358.5	0.06
$Si_{35}H_{32}(C_3H_5O_2)_4$	4.096	289.0	0.02	1.628	359.2	0.05
$Si_{35}H_{28}(C_3H_5O_2)_8$	4.262	289.5	0.01	1.909	360.2	0.03
$Si_{35}H_{24}(C_3H_5O_2)_{12}$	4.181	291.9	0.03	1.189	363.6	0.03
$Si_{35}H_{20}(C_3H_5O_2)_{16}$	3.822	306.4	0.03	1.481	360.6	0.08
$Si_{35}H_{16}(C_3H_5O_2)_{20}$	3.275	316.6	0.04	0.440	364.9	0.04
$Si_{59}H_{60}$	3.648	334.4	0.25	2.894	390.4	0.13
$Si_{59}H_{56}(C_3H_5O_2)_4$	3.539	343.8	0.12	1.064	412.0	0.08
$Si_{59}H_{52}(C_3H_5O_2)_8$	3.515	346.5	0.14	1.051	413.6	0.07

[a] ΔE_1 for ground-state configurations, ΔE_2 for excited-state configurations. [b] f_1 for absorption, f_2 for emission.

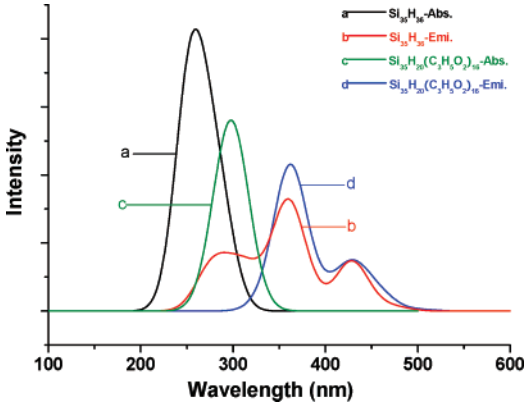

Figure 3. Calculated absorption and emission spectra (see text) for $Si_{35}H_{36}$ and $Si_{35}H_{20}(C_3H_5O_2)_{16}$. The units on the *y*-axis are arbitrary. Fifty roots were calculated, and the peaks were broadened using a Gaussian line shape with a line HWHM (half-width at half-maximum) of 20.

sion peak positions only slightly red-shift. This is consistent with the experimental finding that the PL maximum peak only slightly red-shifts after carboxyl functionalization.[21,24] Moreover, we can see that the HOMO−LUMO energy gap in ground-state configuration is much larger than that in excited-state configuration, mainly because the LUMO energy level moves down significantly and the HOMO energy level moves up remarkably after structure relaxation in excited state. In addition, from the data in Table 2, we can observe that the maximum absorption gap of $Si_{59}H_{56}(C_3H_5O_2)_4$ is about 0.7 eV lower than that of $Si_{35}H_{32}(C_3H_5O_2)_4$, which is consistent with the corresponding gap difference between $Si_{59}H_{60}$ and $Si_{35}H_{36}$ due to the well-known quantum confinement effect. As a result, we can conclude that it is the size of SiQDs, especially the size of the silicon core, that determines the optical properties, while the amounts of adsorbed PA molecules have little effect on the optical spectra.

We further analyzed the simulated absorption and emission spectra of $Si_{35}H_{36}$ and $Si_{35}H_{20}(C_3H_5O_2)_{16}$ (see Figure 3). It could be seen that the PA adsorption leads to a red-shift of about 50 nm on the absorption spectrum, while the emission peak only slightly red-shifts. The absorption peak of $Si_{35}H_{20}(C_3H_5O_2)_{16}$ appears at about 300 nm, which is in good agreement with the experimental values 320 nm[20] and 290

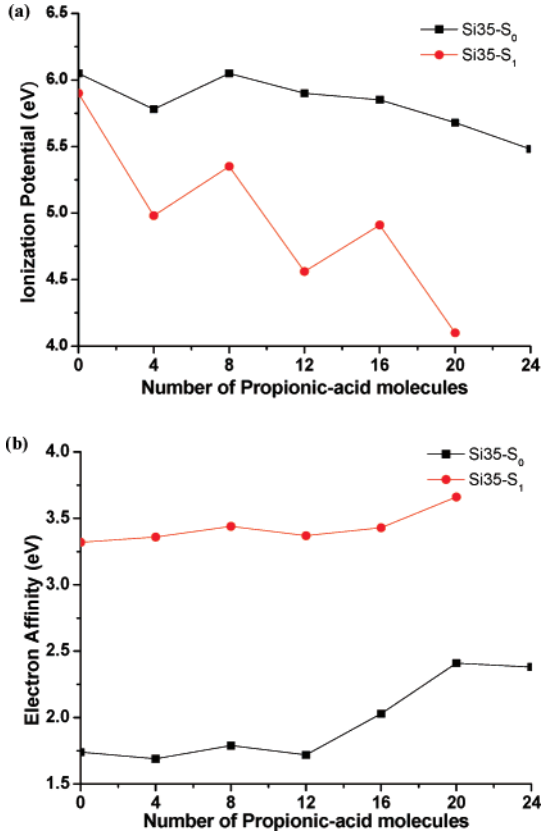

Figure 4. (a) −HOMO energy and (b) −LUMO energy for SiQDs in ground-state (S_0) or excited-state (S_1) configuration (see text) as a function of the adsorbed PA number.

nm.[21] On the other hand, the emission peak of $Si_{35}H_{20}(C_3H_5O_2)_{16}$ appears at around 435 nm, which is close to the experimental value 480 nm in ref 20 but a little far from the experimental value 600 nm in ref 21. This could be explained in terms of different sizes, that is, the diameter of $Si_{35}H_{20}(C_3H_5O_2)_{16}$, 1.1 nm, is close to the size distribution of 1.4 ± 0.3 nm in ref 20 but a little smaller than that of 1.9−2.4 nm in ref 21. Moreover, we find that the optical absorption of $Si_{35}H_{20}(C_3H_5O_2)_{16}$ ranges from 230 nm to 360 nm, while the light emission ranges from 300 nm to 520 nm. Since these spectra show a substantial PL quantum yield in the visible region, it is possible to use PA-terminated SiQDs as candidates of biological chromophores.[55]

3.3. Electronic Properties. In order to gain insight into the physical mechanisms responsible for the optical properties, it is necessary to examine the nature of the electronic states responsible for absorption and emission, that is, the highest occupied molecular orbital (HOMO) and the lowest unoccupied molecular orbital (LUMO). In most occasions, the change in charge density introduced by the excitation of an electron from the HOMO to the LUMO induces forces on each atom due to the changes in the corresponding orbital densities.

In principle, electron affinity (A) corresponds to the energy given by the system when an additional electron is added, while the ionization potential (I) is referred to as the energy provided to the system to remove an electron. Melnikov and Chelikowsky[56] pointed out that for SiQDs LUMO and HOMO energies behave qualitatively as −A and −I, and

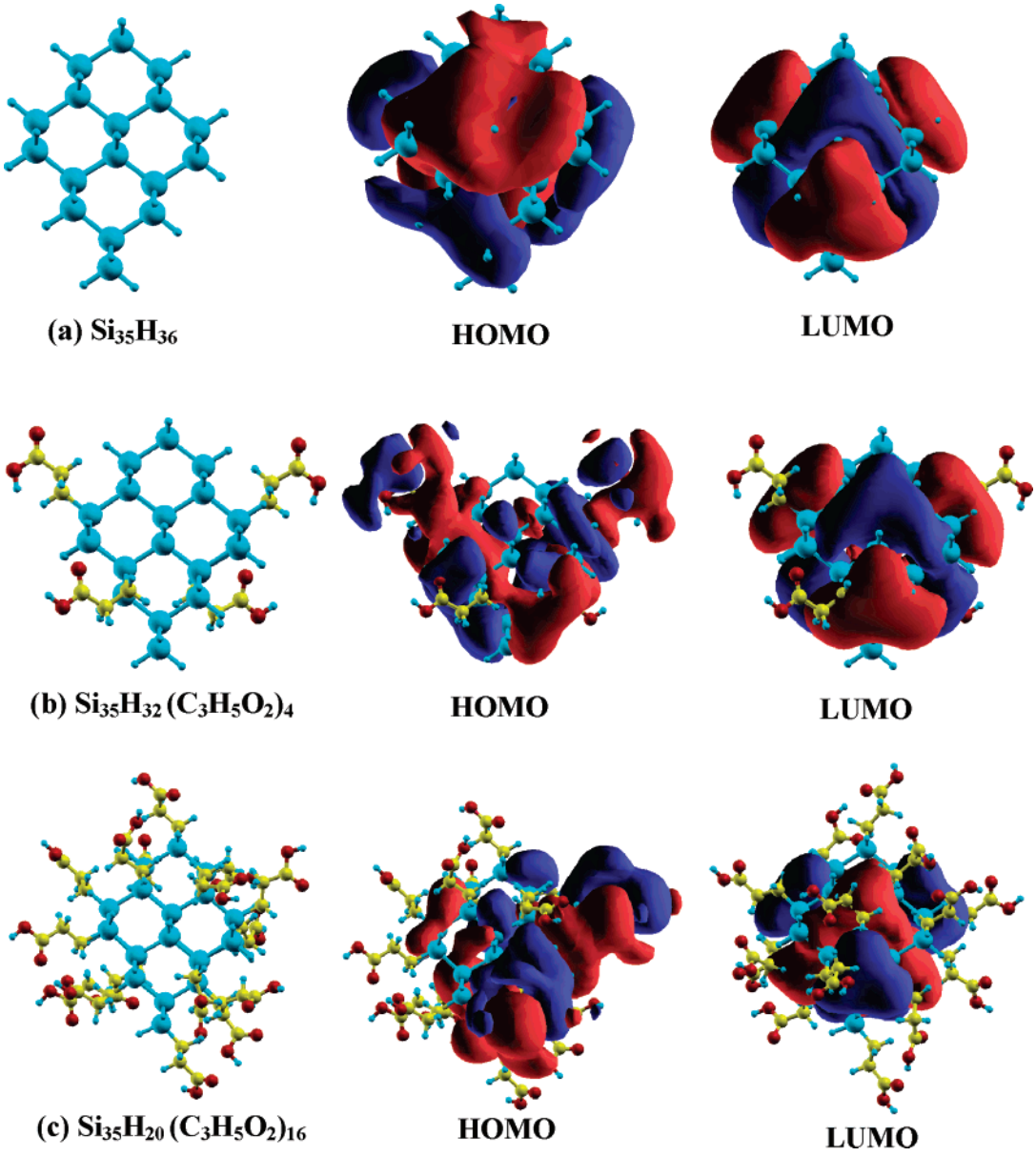

Figure 5. The isosurfaces of the HOMO and LUMO for $Si_{35}H_{36}$, $Si_{35}H_{32}(C_3H_5O_2)_4$, and $Si_{35}H_{20}(C_3H_5O_2)_{16}$ in ground-state configurations.

this theorem has been successfully applied to explore the electronic properties of alkyl-terminated SiQDs.[34] In the subsection, we will discuss the HOMO and LUMO energies and relate them to electron affinity and ionization potentials of PA-terminated SiQDs. In Figure 4, we show the electron affinity and ionization potential of SiQDs as a function of the adsorbed PA number. In Figure 4(a), the ionization potential decreases remarkably with an increase in the adsorbed PA number in the excited-state configuration. In detail, the ionization potential is 5.90 eV for the S_1 state $Si_{35}H_{36}$, while it decreases to 5.35 and 4.10 eV for the S_1 states $Si_{35}H_{28}(C_3H_5O_2)_8$ and $Si_{35}H_{16}(C_3H_5O_2)_{20}$, respectively. This implies that PA-terminated SiQDs possess higher reactivity than that of hydrogenated SiQDs. On the other hand, the LUMO energy is slightly affected by PA adsorption except when the PA number exceeds 12 and the SiQDs are in ground-state configuration, as can be seen in Figure 4(b).

The isosurfaces of HOMO and LUMO orbitals in ground-state configurations of $Si_{35}H_{36}$, $Si_{35}H_{32}(C_3H_5O_2)_4$, and $Si_{35}H_{20}(C_3H_5O_2)_{16}$ are shown in Figure 5. For $Si_{35}H_{36}$, the HOMO is triply degenerated due to the structure with T_d symmetry, while the LUMO is a holosymmetry delocalized orbital belonging to A_1 symmetry. Both HOMO and LUMO of $Si_{35}H_{36}$ are delocalized throughout the core of the silicon cluster. The isosurface of frontier orbitals reflects the structure symmetry and implies the isotropic reactivity of hydrogenated SiQDs. In contrast, for PA-terminated SiQDs, such as $Si_{35}H_{32}(C_3H_5O_2)_4$ and $Si_{35}H_{20}(C_3H_5O_2)_{16}$, the HOMO isosurface is mostly drawn to the surface toward the PA branch, while most of the LUMO isosurface still exists in the core of the cluster, as can be clearly seen in Figure 5(b),-(c). A similar case has been reported by Puzder et al.[47] in studying the optical properties of silicon nanocrystals with oxygen passivation on the surface.

In order to further clarify the difference in the nature of the electronic states caused by PA adsorption, we schematically present the absorption and emission processes of $Si_{35}H_{36}$ and $Si_{35}H_{20}(C_3H_5O_2)_{16}$ in Figure 6. In Figure 6(a), for $Si_{35}H_{36}$

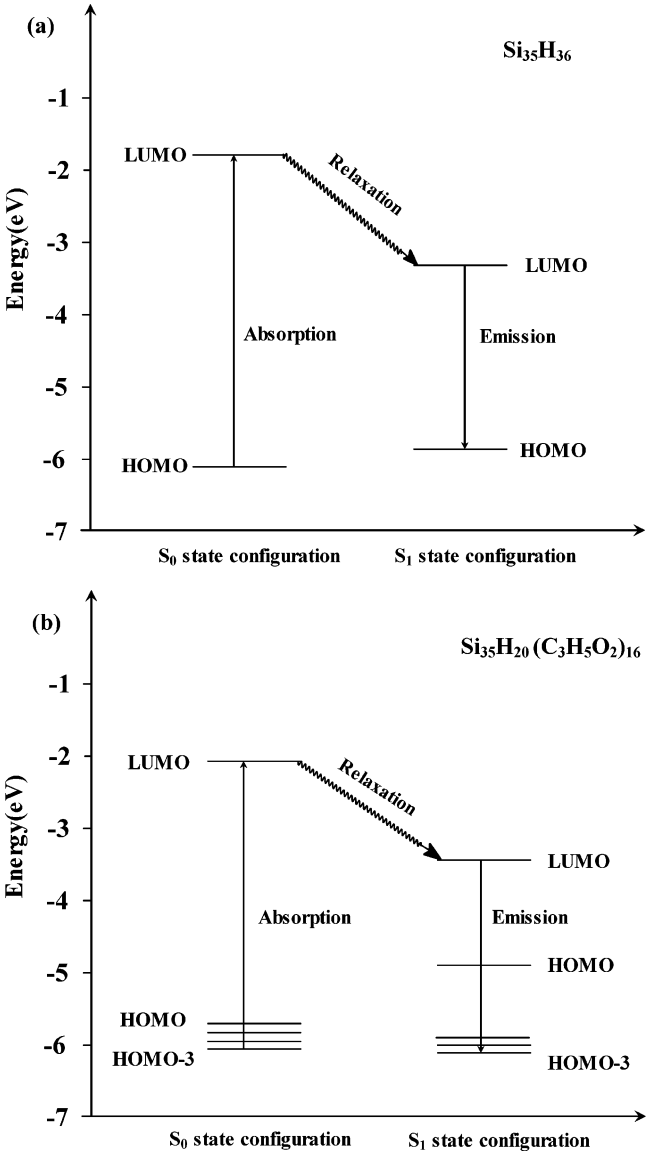

Figure 6. Schematic diagram showing photoabsorption and emission processes for $Si_{35}H_{36}$ and $Si_{35}H_{20}(C_3H_5O_2)_{16}$.

the absorption spectrum is determined by the electron transfer from HOMO to LUMO. In the structure relaxation progress from ground-state configuration in T_d symmetry to excited-state configuration in C_1 symmetry, the energy of LUMO decreases as much as 1.578 eV, while the HOMO only increases slightly in energy and splits into several nearly degenerated orbitals, denoted by HOMO-n (n = 0, 1, 2, or 3) hereafter. The PL emission occurs when the electron transfers from LUMO to HOMO-n (n = 0, 1, 2, or 3) in the excited-state configuration.

The electronic properties of PA-terminated SiQDs are much more complex than those of hydrogenated SiQDs. Figure 6(b) shows the selected frontier orbital energy levels and the PL process of $Si_{35}H_{20}(C_3H_5O_2)_{16}$. Our calculation results reveal that the adsorbed PA molecules result in some new orbitals with adjacent energies around Fermi energy and narrow the HOMO−LUMO energy gap, leading the electronic transition to be much more complex. For example, the absorption corresponding to the peak on the spectrum originates from the electron transfer from HOMO-3 to LUMO, not HOMO to LUMO. In detail, the oscillator strength is 0.03 for HOMO-3 to LUMO electron transfer in $Si_{35}H_{20}(C_3H_5O_2)_{16}$, while the value is only 0.002 for HOMO to LUMO electron transfer. Natural orbital analysis showed that the charge density of $Si_{35}H_{20}(C_3H_5O_2)_{16}$ HOMO-3 delocalized in the silicon core and similar to that of $Si_{35}H_{36}$ HOMO.

In excited-state configuration, the distribution difference of the frontier orbitals between $Si_{35}H_{36}$ and $Si_{35}H_{20}(C_3H_5O_2)_{16}$ is much more evident than that in the ground-state configuration, as can be seen in the right panel of Figure 6. The HOMO energy of $Si_{35}H_{20}(C_3H_5O_2)_{16}$ in the excited-state configuration increases about 0.9 eV compared with that in the ground-state configuration, while the HOMO energy of $Si_{35}H_{36}$ only increases by about 0.15 eV after geometrical relaxation. Figure 7 shows the isosurfaces of the frontier orbitals of $Si_{35}H_{36}$ and $Si_{35}H_{20}(C_3H_5O_2)_{16}$ in excited-state configurations. It could be clearly seen that most of the HOMO is localized in the PA branch, while the pattern of the $Si_{35}H_{20}(C_3H_5O_2)_{16}$ HOMO-3 is generally similar to $Si_{35}H_{36}$ HOMO, though the signs (±) of some orbitals (e.g., denoted by red and blue in the Figure 7) are reversed. As a matter of fact, electron transfer from LUMO to HOMO-3 is proposed to account for the peak on the emission spectrum of $Si_{35}H_{20}(C_3H_5O_2)_{16}$. This means the PA adsorption does not affect the general nature of the optical properties of SiQDs.

Experimentally, the PA adsorption not only increases the dispersibility but also improves the PL stability of the SiQDs against degeneration by water and oxygen.[21] Although this could be simply explained in terms of steric hindrance, the physical mechanism remains unknown. At a molecular level, our calculations reveal that new frontier orbitals (HOMO, HOMO-1, HOMO-2) with energies adjacent to the Fermi energy appear as a result of PA adsorption. Natural orbital analysis showed that these new frontier orbitals are composed of the atomic orbitals on the PA branch. The modified surface of SiQDs can serve as a reaction substrate to oxygen and solvent molecules, which is responsible for the increase in both PL stability and water solubility. Similarly, it is suggested that alkyl passivation weakly affects optical gaps but leads to new bound states that affect excited-state properties of 1−2 nm silicon nanoclusters.[34]

Allylamine (CH_2═$CHCH_2NH_2$)[20] and acrylic acid (CH_2═CHCOOH)[21,23] have been successfully attached to the surface of SiQDs in different experimental conditions, both leading to water-soluble photoluminescent SiQDs. Allylamine and acrylic acid have the same carbon framework and different hydrophilic groups, $-NH_2$ or −COOH. Compared to N (3.04) and O (3.44) atoms, the electronegativity of C (2.55) is closer to that of the Si (1.90).[52] According to our calculation results, in $Si_{35}H_{35}(OH)$ and $Si_{35}H_{35}(NH_2)$, the adsorption groups carry negative charges of −0.130 and −0.175, respectively. Both of them obtain more negative charge than that (−0.06) of the PA molecule. Thus, the charge transfer in Si−CR bond is weaker than that in the Si−NR bond or the Si−OR bond. Recent theoretical calculations[57] also showed that the single Si−C bridges are very stable, and replacing the Si−H bond by alkyl groups (Si−

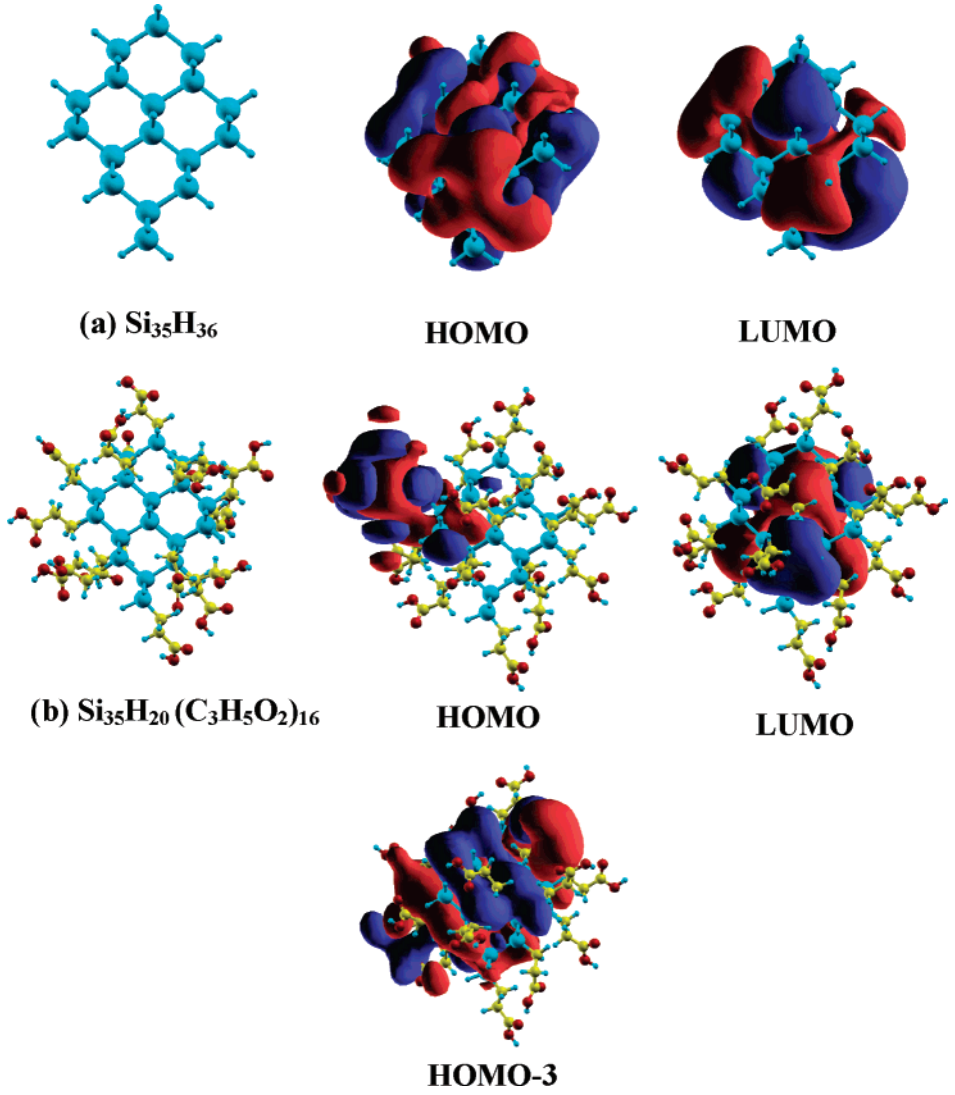

Figure 7. The isosurfaces of the selected frontier orbitals for $Si_{35}H_{36}$ and $Si_{35}H_{20}(C_3H_5O_2)_{16}$ in excited-state configurations.

C−R) results in a small reduction of the energy gap (0.5 eV) as compared to the large reduction observed with an oxide surface termination (2.3 eV).[34] There is no doubt that the formation of the Si−C surface bond will lead to small changes in the electronic and optical characters of the SiQDs. Hence, the PA molecules lead to small changes in the electronic and optical properties of the SiQDs and can be used as ideal branches to help the SiQDs maintain its PL stability.

4. Conclusions

The adsorbed PA molecules slightly affect the geometric structures of the silicon core, while the electron excitation leads to an obvious distortion to the structures. Furthermore, the PA adsorption has little effect on the absorption or emission spectra. It is the size of SiQDs, especially the size of the silicon core that determines the optical properties. The PA adsorption does not change the optical nature of the SiQDs. However, the adsorption substantially decreases the ionization potentials in the excited state and results in new active orbitals with adjacent energies around Fermi energy. Thus, the modified surface of SiQDs can serve as a reaction substrate to oxygen and solvent molecules, which is responsible for the increase in both PL stability and water solubility.

Finally, our study verifies that surface modification is very important for the band structure engineering. Theoretical calculations can illuminate the physical mechanism and chemical nature of many useful materials at molecular or atomic levels.

Acknowledgment. The work described in this paper is supported by the Research Grants Council of Hong Kong SAR [Project Nos. 8730023, CityU 103106, and CityU 3/04C].

References

(1) Buriak, J. M. *Chem. Rev.* **2002**, *102*, 1271.

(2) Hua, F.; Stewart, M. T.; Ruckenstein, E. *Langmuir* **2005**, *21*, 6054.

(3) Dancil, K. P. S.; Greiner, D. P.; Sailor, M. J. *J. Am. Chem. Soc.* **1999**, *121*, 7925.

(4) Sohn, H.; Létant, S.; Sailor, J.; Trogler, W. C. *J. Am. Chem. Soc.* **2000**, *122*, 5399.

(5) Meindl, J. D.; Chen, Q.; Davis, J. E. *Science* **2001**, *293*, 2044.

(6) Veinot, J. G. C. *Chem. Commun.* **2006**, *40*, 4160.

(7) Canham, L. T. *Appl. Phys. Lett.* **1990**, *57*, 1046.

(8) Ruckenstein, E.; Gourisankar, S. V. *J. Colloid. Interface Sci.* **1984**, *101*, 436.

(9) Holmes, J. D.; Ziegler, K. J.; Doty, R. C.; Pell, L. E.; Johnston, K. P.; Korgel, B. A. *J. Am. Chem. Soc.* **2001**, *123*, 3743.

(10) Park, N. M.; Kim, T. S.; Park, S. J. *Appl. Phys. Lett.* **2001**, *78*, 2575.

(11) Kim, B. H.; Cho, C. H.; Kim, T. W.; Park, N. M.; Sung, G. Y. *Appl. Phys. Lett.* **2005**, *86*, 091908.

(12) Nagesha, D. K.; Whitehead, M. A.; Coffer, J. L. *Adv. Mater.* **2005**, *17*, 921.

(13) Canham, L. T.; Reeves, C. L.; Newey, L. P.; Houlton, M. R.; Cox, T. I.; Buriak, J. M; Stewart, M. P. *Adv. Mater.* **1999**, *11*, 1505.

(14) Delerue, C.; Allan, G.; Lannoo, M. *Phys. Rev. B* **1993**, *48*, 11024.

(15) Seotsanyana-Mokhosi, I.; Kuznetsova, N.; Nyokong, T. *J. Photochem. Photobiol., A* **2001**, *140*, 215.

(16) Wolkin, M. V.; Jorne, J.; Fauchet, P. M. *Phys. Rev. Lett.* **1999**, *82*, 197.

(17) Zhou, Z. Y.; Brus, L.; Friesner, R. *Nano Lett.* **2003**, *3*, 163.

(18) Bruchez, M., Jr.; Moronne, M.; Gin, P.; Weiss, S.; Alivisatos, A. P. *Science* **1998**, *281*, 2013.

(19) Yan, C. S.; Bley, R. A.; Kauzlarich, S. M.; Lee, H. W. H.; Delgado, G. R. *J. Am. Chem. Soc.* **1999**, *121*, 5191.

(20) Warner, J. H.; Hoshino, A.; Yamamoto, K.; Tilley, R. D. *Angew. Chem., Int. Ed.* **2005**, *44*, 4550.

(21) Li, Z. F.; Ruckenstein, E. *Nano Lett.* **2004**, *4*, 1463.

(22) Ruckenstein, E.; Li, Z. F. *Adv. Colloid Interface Sci.* **2005**, *113*, 43.

(23) Sato, S.; Swihart, M. T. *Chem. Mater.* **2006**, *18*, 4083.

(24) Rogozhina, E. V.; Eckhoff, D. A.; Gratton, E.; Braun, P. V. *J. Chem. Mater.* **2006**, *16*, 1421.

(25) Stewart, M. P.; Buriak, J. M. *J. Am. Chem. Soc.* **2001**, *123*, 7821.

(26) Lie, L. H.; Patole, S. N.; Pike, A. R.; Ryder, L. C.; Connolly, B. A.; Ward, A. D.; Tuite, E. M.; Houlton, A.; Horrocks, B. R. *Faraday Discuss.* **2004**, *125*, 235.

(27) Chao, Y.; Krishnamurthy, S.; Montalti, M.; Lie, L. H.; Houlton, A.; Horrocks, B. R.; Kjeldgaard, L.; Dhanak, V. R.; Hunt, M. R. C.; Šiller, L. *J. Appl. Phys.* **2005**, *98*, 044316.

(28) Pettigrew, K. A.; Liu, Q.; Power, P. P.; Kauzlarich, S. M. *Chem. Mater.* **2003**, *15*, 4005.

(29) Li, Z. F.; Kang, E. T.; Neoh, K. G.; Tan, K. L. *Biomaterials* **1998**, *19*, 45.

(30) Franchina, J. G.; Lackowski, W. M.; Dermody, D. L.; Crooks, R. M.; Bergbreiter, D. E. *Anal. Chem.* **1999**, *71*, 3133.

(31) Zhang, R. Q.; Costa, J.; Bertran, E. *Phys. Rev. B* **1996**, *53*, 7847.

(32) Zhou, Z.; Friesner, R. A.; Brus, L. *J. Am. Chem. Soc.* **2003**, *125*, 15599.

(33) Reboredo, F. A.; Schwegler, E.; Galli, G. *J. Am. Chem. Soc.* **2003**, *125*, 15243.

(34) Reboredo, F. A.; Galli, G. *J. Phys. Chem. B* **2005**, *109*, 1072.

(35) Wang, X.; Zhang, R. Q.; Niehaus, T. A.; Frauenheim, Th. *J. Phys. Chem. C* **2007**, *111*, 2394.

(36) Porezag, D.; Frauenheim, Th.; Köhler, Th.; Seifert, G.; Kaschner, R. *Phys. Rev. B* **1995**, *51*, 947.

(37) Elstner, M.; Porezag, D.; Jungnickel, G.; Elsner, J.; Haugk, M.; Frauenheim, T.; Suhai, S.; Seifert, G. *Phys. Rev. B* **1998**, *58*, 7260.

(38) Niehaus, T. A.; Suhai, S.; Sala, F. D.; Lugli, P.; Elstner, M.; Seifert, G.; Frauenheim, Th. *Phys. Rev. B* **2001**, *63*, 085108.

(39) Casida, M. E.; Casida, K. C.; Salahub, D. R. *Int. J. Quantum Chem.* **1998**, *70*, 933.

(40) Casida, M. E.; Salahub. D. R. *J. Chem. Phys.* **2000**, *113*, 8918.

(41) Fehér, F. *Research Report of the Federal State North Rhine-Westphalia*; West-deutscher Verlag: Köln, 1977.

(42) Zdetsis, A. D. *Rev. Adv. Mater. Sci.* **2006**, *11*, 56.

(43) Luppi, E.; Degoli, E.; Cantele, G.; Ossicini, S.; Magri, R.; Ninno, D.; Bisi, O.; Pulci, O.; Onida, G.; Gatti, M.; Incze, A.; Sole, E. D. *Opt. Mater.* **2005**, *27*, 1008.

(44) Williamson, A. J.; Grossman, J. C.; Hood, R. Q.; Puzder, A.; Galli, G. *Phys. Rev. Lett.* **2002**, *89*, 196803.

(45) Vasiliev, I.; Ogut, S.; Chelikowsky, J. R. *Phys. Rev. Lett.* **2001**, *86*, 1813.

(46) Garoufalis, C. S.; Zdetsis, D.; Grimme, S. *Phys. Rev. Lett.* **2001**, *87*, 276402.

(47) Puzder, A.; Williamson, A. J.; Grossman, J. C.; Galli, G. *J. Am. Chem. Soc.* **2003**, *125*, 2786.

(48) Garoufalis, C. S.; Zdetsis, A. D. *Phys. Chem. Chem. Phys.* **2006**, *8*, 808.

(49) Vasiliev, I.; Chelikowsky, J. R.; Martin, R. M. *Phys. Rev. B* **2002**, *65*, 121302.

(50) Luppi, M.; Ossicini, S. *Phys. Rev. B* **2005**, *71*, 035340.

(51) *CRC Handbook of Chemistry and Physics*, 78th ed.; Lide, D. R., Ed.; CRC Press: New York, 1997; pp 9−22.

(52) Stuhlmann, C.; Bogdányi, G.; Ibach, H. *Phys. Rev. B* **1992**, *45*, 6786.

(53) *The Nature of the Chemical Bond and the Structure of Molecules and Crystals*; Pauling, L., Ed.; Cornell University Press: 1960.

(54) Schafer, R.; Becker, J. A. *Phys. Rev. B* **1996**, *54*, 10296.

(55) Wilson, W. L.; Szajowski, P. F.; Brus, L. E. *Science* **1993**, *262*, 1242.

(56) Melnikov, D. V.; Chelikowsky, J. R. *Phys. Rev. B* **2004**, *69*, 113305.

(57) Cucinotta, C. S.; Bonferroni, B.; Ferretti, A.; Ruini, A.; Caldas, M. J.; Molinari, E. *Surf. Sci.* **2006**, *600*, 3892.

CT700041V